Research in Astron. Astrophys. **2011** Vol. **11** No. **1**, 43–62
http://www.raa-journal.org *http://www.iop.org/journals/raa*

***R**esearch in*
***A**stronomy and*
***A**strophysics*

A possible precession period for superluminal ejection in QSO 3C 279

Shan-Jie Qian

National Astronomical Observatories, Chinese Academy of Sciences, Beijing 100012, China;
rqsj@bao.ac.cn

Received 2010 April 15; accepted 2010 June 22

Abstract The search for periodic features in flux variability and superluminal ejection in blazars has been an important subject, which is helpful for providing significant clues to the understanding of the structure and kinematics of relativistic jets (physical processes of acceleration and collimation) and their association with central energy engines (black hole/accretion disk systems). The wobbling of the ejection position angle of VLBI knots in superluminal sources has been interpreted in terms of the precession of the jet ejection nozzle as one of the alternative interpretations. We study the change with time of the initial position angle of superluminal knots in QSO 3C 279, using VLBI-data collected from the literature spanning more than $\sim$30 yr and propose a jet-nozzle precession model which has very small viewing angles (less than 2°) to fit the long-term trends in both variations in the inner-jet position angle (Chatterjee et al.) and the ejection position angle of the VLBI components. It is shown that an ejection-nozzle precession period of $\sim$25 yr could be appropriate to fit the long-term trend in the variation of the ejection position angle. However, the short-term swings and fluctuations in the ejection position angle cause some uncertainties. We also fit a model to the trajectory of component C4, correcting its non-ballistic motion near the core.

Key words: radio continuum — quasars — jets — kinematics — individual: 3C 279

1 INTRODUCTION

QSO 3C 279 ($z = 0.538$) is one of the most well studied prominent blazars (flat-spectrum compact radio sources with superluminal motion), an optically violent variable (OVV) with large and rapid polarized outbursts. It radiates across the entire electromagnetic spectrum from radio through optical and X-ray to γ-ray. Very strong variability is observed in all these wavebands with various timescales (hours/days to years). 3C 279 is one of the brightest EGRET quasars (Hartman et al. 1992). Multifrequency observations and the study of correlations between different wavebands have demonstrated important clues to the radiation mechanisms, especially for X-ray and γ-ray radiation (Marscher 2008, 2009).

3C 279 is the first object in which apparent superluminal motion was detected in 1971 (Whitney et al. 1971; Cohen et al. 1971). Since then, its mas-scale structure and kinematics have been monitored with very long baseline interferometry (VLBI). Numerous data have been presented in literature on the kinematics of the superluminal knots. VLBI observations reveal that bright components

(knots) are consistently ejected from a core (presumed to be stationary) and move away from it with apparent superluminal speeds ($\sim$4–16c, Chatterjee et al. 2008; Larionov et al. 2008; Jorstad & Marscher 2005; Jorstad et al. 2004; Unwin et al. 1989; Homan et al. 2003; Wehrle et al. 2001; Carrara et al. 1993). Apparent superluminal motion results from relativistic motion of the knots at small viewing angles and their flux density or luminosity is strongly Doppler-boosted.

In recent years, the change of position angle of superluminal ejection in blazars has called for more scrutiny (for example, see Klare et al. 2005; Klare 2003; Valtonen et al. 2008, 2006; Kudryavtseva & Pyatunina 2006; Qian et al. 2007; Agudo et al. 2007). In particular, Qian et al. (2009) have discussed the rotation of the ejection position angle of superluminal knots in QSO 3C 345 and found that there could exist a steady helical channel along which the superluminal components are consistently ejected from the core. Their model-fits show that the channel is precessing with a period of 6.9 yr (in the observer's frame), causing the observed rotation of the ejection position angle of the knots. In addition, different knots have different initial trajectories on the sky-plane.

For the quasar 3C 279, Jorstad & Marscher (2005) show that the ejection position angle of knot C4 and of knots C8 through C20 appears to continuously change from $\sim -114^\circ$ to $\sim -160^\circ$. This trend is more prominently revealed in the change of the inner-jet position angle given in Chatterjee et al. (2008, see the bottom panel of their fig. 6), which contains more VLBI data from 1996 till 2006. From figure 6 of Chatterjee et al. and earlier VLBI data (for example, see Homan et al. 2003 and Abraham & Carrara 1998), it can be shown that the ejection position angle of the superluminal components has slowly decreased from $\sim -100^\circ$ in the 1980s to $\sim -150^\circ$ in 2003, and then rapidly increased to $\sim -120^\circ$ in 2006.

Ten years ago, Abraham & Carrara (1998) proposed a precession model to explain the kinematic behavior (changes in ejection position angle and apparent speed) of components C1 to C5. It will be seen below that this model cannot be applied to consistently interpret the VLBI data presently available for the superluminal components C3 to C24. Thus, more detailed analysis of the VLBI data is needed.

2 COMMENTS ON VLBI RESULTS

In the following, we will argue that it is possible to find a precession model to fit the long-term change in the ejection (or initial) position angle of the superluminal knots observed in QSO 3C 279. However, before proposing our model, we will first make some comments on the results derived from the VLBI observations since the 1970s.

Recently, many works have studied the kinematics of the relativistic jet in 3C 279 (change in the ejection position angle, trajectories of the superluminal knots and their apparent speeds). Correlations of radio variations with the variations of γ-ray, X-ray and optical emissions have also been intensively studied. (see Marscher 2008; Chatterjee et al. 2008; Larionov et al. 2008; Homan et al. 2003; Wehrle et al. 2001; Jorstad & Marscher 2005; Jorstad et al. 2005; Jorstad et al. 2004).

(1) From VLBA (Very Long Baseline Array) observations at 43GHz (1996–2006), Chatterjee et al. (2008) derived the average position angles within 1 mas of the core and the ejection times for the superluminal knots C8 to C23 when their core distances are zero; These data (see their table 5) indicate changes of the ejection position angle (PA) of these knots: the minimum PA is for knot C20 at $\sim -155^\circ \pm 10^\circ$ and the maximum PA for C22 and C23 is at $-102^\circ \pm 17^\circ$ (with a large observational error) and $-114^\circ \pm 5^\circ$, respectively. Larionov et al. (2008) have studied the kinematics of knot C24, showing its ejection position angle of $\sim -120^\circ$ is similar to that for C22–C23. Here we should point out that, in a strict sense, the average position angles given above are not the initial ejection position angles which will be model-fitted for initial non-ballistic motions. However, in this paper we will take these position angles as approximately representing the change in the initial ejection position angles.

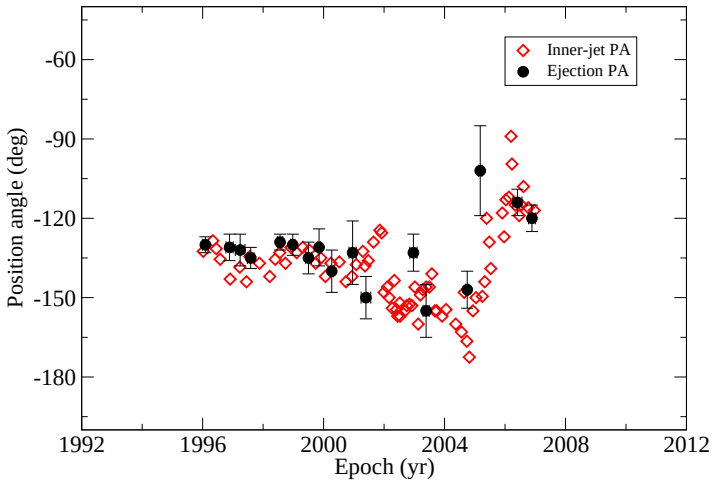

Fig. 1 Comparison between the inner-jet position angles and the ejection position angles of knots C8 to C24 (averaged within 1 mas). VLBI data are from Chatterjee et al. (2008) and Larionov et al. (2008).

In addition, Jorstad & Marscher (2005) more clearly show that the ejection position angle appears to be continuously changing for knots C4 through C20 (see their fig. 1, right panel).

Also, Chatterjee et al. (2008) have discussed the variation of the position angle of the inner jet, which is defined as that of the brightest component within 0.1–0.3 mas of the core. These data clearly show that the position angle of the inner jet changes significantly (between $\sim -170^\circ$ to $\sim -90^\circ$) over the 10 yr (1996–2006) of study (see the bottom panel of their fig. 6). In Figure 1 we show the comparison between the changes in the inner-jet position angle and the ejection position angle during the period 1996–2006. It can be seen that there are short-term position angle swings (jumps and drops) with time-scales of $\leq \sim$0.5–1.0 yr, superimposed on the long-term variations of the inner-jet position angle; for example, within the periods between 2001 and 2002, 2004 and 2005, 2005 and 2006, and 2006 and 2007 with swing amplitudes are $\sim 30^\circ$. It seems that there are also some oscillating fluctuations with a timescale of about 2 yr in the inner-jet position angle, for example in the period between 1996 and 2000.

The short-term swings of the inner-jet position angle might be related to some unusual events (like core motion, non-ballistic motion of superluminal knots and appearance of strong stationary components), and the oscillating fluctuation could be induced by instabilities. If we neglect these swings and oscillating fluctuations, it can be seen from Figure 1 that the long-term trend of the change in inner-jet position angle is similar to that of the change in the ejection position angle (averaged within 1 mas). That is, both the variation of the inner jet position angle and the variation of the ejection position angle roughly or approximately have a similar long-term trend: a slow variation from $\sim$1996 to 2005 with the position angle decreasing from $\sim -130^\circ$ to $\sim -160^\circ$ and a faster variation from $\sim$2005 to $\sim$2007 with the position angle increasing from $\sim -160^\circ$ to $\sim -110^\circ$. We should emphasize that the asymmetry in the time-interval of the slow-variation and fast-variation could be a sign of a precession of the jet-nozzle (see Qian et al. 2007, 2009 and Fig. 5 below).

In addition, in the literature there are data for the ejection times and ejection position angles for knots C3 (Unwin et al. 1989), C4 (Wehrle et al. 2001; Homan et al. 2003), C5 (Carrara et al. 1993), C5a, C6 and C7 (Wehrle et al. 2001). These data are also useful for extending the trend of the ejection position angle variation back to earlier epochs to determine the precession period and test the precession model proposed below. For example, the ejection position angle for knot C5 is $\sim -84^\circ \pm 10^\circ$ (ejection epoch 1984.7$\pm$1, Abraham & Carrara 1998) and might be regarded as the maximum PA of ejection; then we would predict that in the near future ($\sim$2010–2012) the ejection PA would approach $\sim -90^\circ \pm 10^\circ$, if the precession period is about 20–30 yr.

(2) Abraham & Carrara (1998) proposed a precession model with a precession period of 22-years for interpreting the variation in the ejection position angle and apparent speeds of knots C1, C3, C4 and C5. However, recent VLBI observations (Homan et al. 2003; Jorstad et al. 2004, 2005; Jorstad & Marscher 2005; Chatterjee et al. 2008 and references therein) cannot be consistent with the predictions from the model. We find that the model parameters they used are not appropriate to fit the kinematics of the superluminal knots in 3C 279. For example, the angle between the precession axis and the line of sight and the opening angle of the precession cone were chosen in that paper to be 21.5° and 31.4° respectively. (The viewing angle of the ejection direction of the jet varies between 5.8° and 37.2°). Thus, the time-interval from the maximum position angle to the minimum position angle is much larger than the time-interval from the minimum position angle to the maximum position angle (the ratio of the time-intervals is about 20:1). (see Abraham & Carrara 1998, their fig. 1). In fact, the viewing angle of the jet direction derived from recent VLBI observations is between $\sim 0.5^\circ$ and $\sim 2^\circ$. Correspondingly, the ratio of the time-intervals could be much smaller than that given above (It could be $\sim$2:1. See Fig. 1 and Figs. 9–14 below). We may notice that in the framework of nozzle precession for explaining the wobbling of the ejection position angle of superluminal knots, the asymmetry of the time-interval for the slow variation and fast variation of ejection position angle is an important parameter for choosing the parameters of a precession model.

(3) Homan et al. (2003) have made a detailed study of the kinematics of knot C4 at distances from $\sim$2.5 mas to 5 mas. They found that its apparent speed and projected trajectory changed in $\sim$1998.2: prior to 1998.2 the angular velocity was 0.25 mas/yr along a position angle of $\sim -114^\circ$ and after 1998.2 its angular velocity was 0.40 mas yr^{-1} along a position angle of $\sim -140^\circ$. That is, the projected trajectory changed by 26°. Jorstad & Marscher (2005) also showed that component C4 experienced a change of trajectory which finally focuses its path into the direction $\sim -125^\circ$. Homan et al. (2003) pointed out that both the increase of the apparent speed and the change of the trajectory are due to a change in the viewing angle of the knot with its intrinsic speed (or Lorentz factor) being constant along a bent path. They estimated its bulk Lorentz factor $\Gamma \gtrsim 15$ with its viewing angle increasing at the bend from $\lesssim 1^\circ$ to $\lesssim 2^\circ$. This interpretation is consistent with the variation in flux density of the knot, the change in apparent speed and in the projected position angle. We would point out here that this choice of the parameters for knot C4 is an important result for the superluminal motion in 3C 279. Our precession model given below is consistent with this interpretation by Homan et al. (2003), i.e. the superluminal knots in 3C 279 are moving along trajectories with very small viewing angles ($\sim 0.5^\circ$–2°, see below Figs. 5 and 6). In addition, the angle between the precession axis and the line of sight is also very small (only $\sim 1.3^\circ$) and the opening angle of the precession cone is $\sim 1.6^\circ$.

(4) We also point out that the position angle $\sim -114^\circ$ derived for knot C4 prior to 1998.2 at core distances of $\sim$1.0 to 3.0 mas (Homan et al. 2003) does not necessarily mean its ejection position angle is -114°. Actually, from figure 2 of Jorstad et al. (2004), it can be seen that the trajectories of the knots have moved toward the south beyond core-distance $\sim$0.5 mas. It can also be seen that within $\sim$ 0.1 mas, a collimation of the jet could have occurred, thus the initial ejection position angles of the knots could be different from their position angles at large distances (beyond, for example, $\sim$1 mas). Non-ballistic motion has been observed in several knots when they are

near the core. For example, Larionov et al. (2008) have observed significant non-ballistic motion of knot C23 near the core. This could be related to the jet-collimation process at the innermost VLBI-scales. In fact, in the following precession model, we find that the ejection position angle of knot C4 is about -95° which approaches -114° at core-distances >1 mas, as observed (Wehrle et al. 2001; Homan et al. 2003). It will be shown below that when its non-ballistic motion near the core is taken into account, the initial ejection position angle of C4 can then be well fitted by the jet-nozzle procession model with a period of 25 yr.

(5) Some authors tried to search for the correlation of the ejection position angle with the apparent speeds of the superluminal knots in 3C 279, and then estimated the precession period and Lorentz factor. For example, Jorstad & Marscher (2005) showed that for knots C8 to C20, the apparent speed increases from $\sim 5c$ to $\sim 21c$ and then decreases to $\sim 7c$. Considering that a similar high speed ($\sim 15c$) has been detected by Cotton et al. (1979) for knot C1, which was ejected in $\sim$1968, they suggested a jet precession period of $\sim$31 yr and a constant Lorentz factor $\Gamma\sim$21. They pointed out that a precession model with a constant bulk Lorentz factor might explain the observed variation in apparent speed and trajectory of superluminal knots; two or more cycles are needed to confirm its presence. Jorstad & Marscher (2005) suggested that a precession period of $\sim$31 yr predicts a minimum in apparent speed of the jet flow in 2007 similar to the apparent speed of knot C3 found by Unwin et al. (1989) and this should be tested by observations. However, for knots C23 and C24 (ejection epochs 2006.41 and 2006.89 respectively, Larionov et al. 2008) the observed apparent speed is $16.5c$ and $14.7c$ respectively, obviously inconsistent with this prediction. In addition, from figure 5 of Chatterjee et al. (2008), it can be seen that for knots C8 to C23 the apparent speed of these knots (i.e. the slope of the linear fits to the relation of core-distance as a function of time) does not show a regular pattern of variation. As Qian et al. (2007) have suggested, the intrinsic Lorentz factor of knots could be related to the accretion rate of the central black hole and the transformation of electromagnetic energy to bulk motion, which thus could be different for different knots. In addition, when the correlation of optical and X-ray flares with the ejection of superluminal knots is studied, we would also have to recognize their production in different regions in the jet, which possibly have different Doppler factors. Whether there is a periodic behavior in the apparent speed of the knots in 3C 279 remains an open question.

(6) Finally, we would make a comment on the short-term position angle swings (jumps or drops) which severely 'interfere' with the otherwise (presumably) regular pattern of the position angle change with time (see Fig. 1). It can be seen from figures 5 and 6 of Chatterjee et al. (2008) that the short-term position angle swings might be due to: (1) motion of the 'true' core (as a stable reference point) along the jet; (2) non-ballistic motion of superluminal knots; (3) change in the relative brightness of different components leading to the brightest one shifting between different knots; (4) appearance of strong stationary components. In the case of 3C 279, this phenomenon was particularly significant. For example, in the period 2006.0–2006.6, strong stationary components were present.

Since the inner-jet position angles were defined by Chatterjee et al. (2008) to be those of the brightest component within 0.1–0.3 mas of the core, they should depend on the "true" position of the core. In addition, from their figures 6 and 8, it can be found that the short-term position angle swings usually occurred when the 43 GHz core flux varied significantly: for example, the position angle jumps in 2002 and 2006 occurred at a high state of the core's 43 GHz flux density, but the gradual upswing in 2001 occurred at a low state of the core's 43-GHz flux density. The variation of the core's flux density might be related to the change of the core's structure. Marscher (2008) suggests that the core could be at the end of the jet (nozzle) or the first stationary shock, both of which could move during ejections of superluminal knots. Relativistic gas dynamics of jets shows that stationary shocks can be formed at a core distance of a few pc (Daly & Marscher 1988). In the case of 3C 279, due to the very small viewing angle, motion of

the core on such scales along the jet could have projected core distances less than $\sim$0.07 mas, significantly less than the resolution of the 43GHz VLBI observations (0.14 mas$\times$0.38 mas, see Chatterjee et al. 2008), which would not be detected by available VLBI observations. Thus, VLBI astrometric observations of the core motion in 3C 279, like those for the core of 3C 345 (Bartel et al. 1986), relative to near stationary objects would be very helpful. In addition, due to non-ballistic motion near the core (jet-collimation could occur at projected core distance less than $\sim$0.1 mas), the measured position angles at core-distances larger than $\sim$0.2 mas might not represent their initial (true) ejection position angles. This makes it difficult to derive the accurate pattern of position angle change with time. In fact, in literature, few VLBI data give accurate position angles of the knots within core-distances less than 0.1–0.2 mas and their real errors in the measured position angles could be much larger than their face-on values given in VLBI observational reports. For example, in Chatterjee et al. (2008), position angles for C8 to C23 are given only in terms of the average values within 1 mas and Jorstad et al. (2004) give the position angles for knots C7a to C16 only in terms of their mean values within 0.5 mas, thus smoothing out all the effects of non-ballistic motion.

In summary, by commenting on the available VLBI observation results from 1972 to 2007, we find that the variation in position angle of superluminal components with time in 3C 279 is extremely complicated. It may consist of: (1) long-term changes with timescales of $\sim$20–30 yr; (2) oscillations (or fluctuations) with timescales of $\sim$2 yr; (3) short-term swings (jumps and drops) with timescales of $\sim$0.5 yr. Therefore it is extremely difficult to explain this behavior by simple models, especially in terms of the regular PA-change pattern of jet-precession models. It is possible that the variation of the ejection position angle of the superluminal components is non-regular (non-periodic): it stays constant and sometimes slowly decreases (as in the period 1998–2005) or abruptly increases (as in the period of 2005–2007). However, the trend of the position angle variation in the period between 1998–2007 also seems to show some inklings of nozzle precession. Thus in the present paper, we will try to establish a jet-nozzle precession model with very small viewing angles ($\theta \leq 2^\circ$) to fit the long-term trend of the change in the ejection position angle. This work may solely be regarded as a trial test to check to what extent a jet-nozzle precession model could be applicable for the variation in the ejection position angle of superluminal knots in 3C 279. Space mm-VLBI measurements would be helpful for determining the ejection position angle of knots in 3C 279 at core-distances less than 0.1 mas where the ejection position angle could be determined more accurately.

In the following, we will use both the data on inner jet position angle and ejection position angle, which are complementary to each other, to show the precession behavior. In this paper, we will adopt the concordant cosmological model with Ω_Λ=0.7, Ω_m=0.3 and Hubble constant H_0=70 km s^{-1} Mpc^{-1} (Spergel et al. 2003). Thus for 3C 279, $z = 0.538$, its luminosity distance is $D_{\rm L} = 3.096$ Gpc (Hogg 1999; Pen 1999) and angular distance $D_{\rm A}$=1.309 Gpc. Angular scale 1 mas=6.35 pc and proper motion of 1 mas yr^{-1} is equivalent to an apparent velocity of 31.81c.

3 FORMULISM OF THE MODEL

In order to develop our precession model for the superluminal ejection of the knots in 3C 279, we first describe the formulism (following Qian et al. 1991, 2009). The geometry of the model is shown in Figure 2, in which the coordinate system (X_p, Y_p, Z_p) has the Y_p-axis directed toward the observer, i.e. the plane (X_p, Z_p) is defined as the sky plane. In this plane, the Z_n-axis is defined as the direction toward the north pole and the X_n-axis as opposite to the direction of right ascension. The observed position angle of VLBI knots is measured clockwise from the Z_n-axis. We define a third coordinate system (X, Y, Z): the X-axis coincides with axis X_p and the Z-axis is situated in the Y_p-Z_p plane forming an angle ε with the Y_p-axis. The Z-axis is defined as the precession axis and the precession cone has a half opening angle of η.

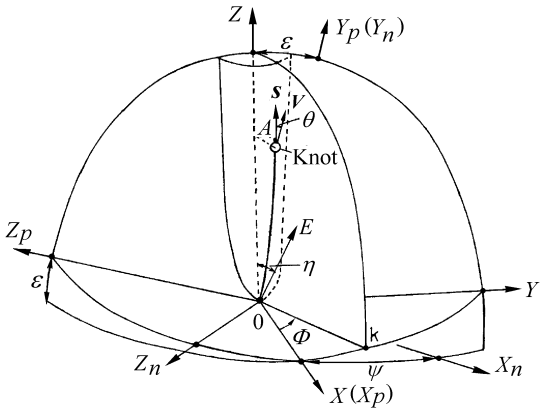

Fig. 2 Geometry of the coordinate system. Here θ denotes the angle between the knot's velocity vector and the direction toward the observer.

In the case of quasar 3C 279, we will assume that the superluminal knots move along individual collimated trajectories, which are defined by parameters in cylindrical coordinates (z, A, Φ), as shown in Figure 2. $\boldsymbol{S}$ denotes the direction of the speed vector, $\boldsymbol{V}$ denotes the direction toward the observer (parallel to direction Y_p) and θ denotes the viewing angle of the knot.

As in the case of quasar 3C 345 (Qian et al. 2009), we assume that each of the VLBI knots moves along a curved trajectory with a constant phase (Φ=constant), but for successive knots, the phase is changed by precession. (Their individual curved (or collimated) trajectories will be described below). A curved trajectory is defined by parameters $(A(z), \Phi)$, which describe the amplitude and phase respectively. Thus, a trajectory can be described in the (X, Y, Z) system as follows:

$$X(z, \Phi) = A(z)\cos\Phi, \tag{1}$$

$$Y(z, \Phi) = A(z)\sin\Phi, \tag{2}$$

$$Z(z) = z. \tag{3}$$

The projection of the trajectory on the sky plane is represented by

$$X_n(z, \Phi) = X_p(z, \Phi)\cos\psi - Z_p(z, \Phi)\sin\psi, \tag{4}$$

$$Z_n(z, \Phi) = X_p(z, \Phi)\sin\psi + Z_p(z, \Phi)\cos\psi, \tag{5}$$

where ψ is the angle between the $X(X_p)$-axis and the X_n-axis,

$$X_p(z, \Phi) = X(z, \Phi), \tag{6}$$

$$Z_p(z, \Phi) = Z(z)\sin\varepsilon - Y(z, \Phi)\cos\varepsilon. \tag{7}$$

We give the formulae for viewing angle θ, Doppler factor δ, apparent transverse velocity β_a and elapsed time T' after ejection as follows.

(1) Viewing angle θ

$$\theta = \arccos[\cos\varepsilon(\cos\Delta + \sin\varepsilon\tan\Delta_p)], \tag{8}$$

where

$$\Delta = \arctan\left[\left(\frac{dX}{dZ}\right)^2 + \left(\frac{dY}{dZ}\right)^2\right]^{1/2}. \tag{9}$$

Δ is the angle between the spatial velocity vector and Z-axis, and

$$\Delta_p = \arctan\left(\frac{dY}{dZ}\right) \tag{10}$$

is the projection of Δ on the (Y, Z)-plane.

(2) Apparent transverse velocity $v_{\rm a}$ and Doppler factor δ

$$v_{\rm a} = c\beta_{\rm a} = \frac{c\beta\sin\theta}{1-\beta\cos\theta}\,, \tag{11}$$

and

$$\delta = \frac{1}{\Gamma(1-\beta\cos\theta)}\,, \tag{12}$$

where β=$\frac{v}{c}$, v is the spatial velocity of the knot, and Γ=$(1-\beta^2)^{-1/2}$ is the Lorentz factor.

(3) Elapsed time T', at which the knot reaches axial distance z'

$$T' = \int_0^{z'} \frac{1+z}{\Gamma\delta v\cos\Delta_s} dz', \tag{13}$$

where z represents the redshift of 3C 279 and

$$\Delta_s = \arccos\left[\left(\frac{dX}{dz}\right)^2 + \left(\frac{dY}{dz}\right)^2 + 1\right]^{-1/2}, \tag{14}$$

and Δ_s is the instantaneous angle between the velocity vector and the Z-axis.

All coordinates and amplitude $A(z)$ are measured in units of mas.

4 COLLIMATED TRAJECTORY AND PARAMETERS CHOSEN

Qian et al. (2009) have recently proposed a precession model to explain the change of initial ejection position angle of the superluminal knots in QSO 3C 345. Here we follow the line of thought of that paper (also see Qian et al. 1991) to propose a new model for QSO 3C 279. Our precession model for 3C 279 is different from simple ballistic models, showing individual superluminal knots moving along collimated trajectories, not along straight lines after ejection.

In order to fit the observed (initial) ejection position angle of the superluminal knots in 3C 279 by a precession model, we would try to find an appropriate set of model parameters and functions to describe the amplitude and phase of the collimated jet. We will assume that each knot moves along a collimated trajectory which has a constant phase Φ with its amplitude varying along the precession axis. However, different knots have their own phase Φ which is precessing with time, causing the ejection position angle of knots to vary with time.

In the case of 3C 279, in contrast to 3C 345 (Qian et al. 2009), the short-term position angle swings of the jet is a problem, contaminating the otherwise presumably regular variation pattern. These swings are apparent in figure 6 of Chatterjee et al. (2008) for the change of the inner-jet position angle with time: for example, the position–angle swings in time-intervals 2001.9–2002.0, 2004.8–2004.9, 2005.3–2005.4 and 2006.1–2006.2 (with ΔPA$\sim$20°–30°). These short-term swings of position angle possibly (sometimes) 'blur' the regular variation of the ejection position angle of knots.

In addition, 3C 279 is a very active source in which ejection of knots is very frequent, and a number of components cannot be identified as superluminal knots; some of them are stationary. These factors also lead to difficulties in identification of the sequence of observed superluminal knots. However, the evolution of the position angle of the inner jet of 3C 279 given by Chatterjee

et al. (2008) has a clear trend: during the period from 1996 to 2007, the position angle gradually decreases from $\sim -130^\circ$ to a minimum at $\sim -160^\circ$ at epoch 2003–2004, and then rapidly increases to $\sim -110^\circ$ at epoch 2007. This pattern indicates the large asymmetry of the variation of position angle of the inner jet. As we will see, this asymmetry could be a significant signal for a precession process and is caused by precession if both the viewing angle of the jet and the opening angle of the precession cone are very small.

Although the ejection of the superluminal knots in 3C 279 has a rather wide range of position angles, each of the components experiences a change of trajectory that focuses its path into the direction of $\sim -125^\circ$ at core-distances larger than about 1 mas (Jorstad et al. 2004; Jorstad & Marscher 2005; Homan et al. 2003). Thus, the superluminal knots in 3C 279 should move along collimated trajectories. In order to choose the shape of the collimated trajectory of the knots, we would have to take into account the maximum separation between the trajectories. The observed separation between the trajectory of C4 and that of C9 at a core distance $\gtrsim$1 mas is about 0.5 mas (Jorstad et al. 2004; Homan et al. 2003). In our model (see below) we assume that the maximum separation between the two extreme trajectories is slightly larger than this value. In Figure 5, the maximum separation corresponds to a difference of precession phase $\sim$4.3 rad and $\sim$2 rad.

In addition, we should choose an appropriate formulism to describe the collimation of the trajectory. Based on the above arguments, we chose the collimated trajectory to be described as follows.

The amplitude $A(z)$ of the collimated trajectory as a function of z is taken as follows: when $z \leq b$,

$$A(z) = 1.375{\times}10^{-2}\frac{2b}{\pi}\sin\left(\frac{\pi z}{2b}\right), \tag{15}$$

and when $z > b$,

$$A(z) = 1.375 \times 10^{-2}\frac{2b}{\pi}. \tag{16}$$

Parameter b may be regarded as a 'collimation parameter' to describe the pattern of jet collimation. Its value can be determined from the model-fitting to the kinematics of individual superluminal knots (their trajectory, core-distance and apparent speed; we will give the results of these fittings for several superluminal knots in a separate paper). The phase Φ is defined by parameter ϕ for a specific trajectory as

$$\Phi = \phi + \Phi_0, \tag{17}$$

Φ_0 is a constant taken as 3.783 rad and ϕ is defined as the precession phase.

This form of the trajectory is a simplified way to describe a collimated jet and is easier to calculate.

Thus when $z \leq b$,

$$\frac{dA}{dz} = 1.375 \times 10^{-2}\cos\left(\frac{\pi z}{2b}\right). \tag{18}$$

This implies that the initial precession cone has a half opening angle equal to $\eta = 0.79^\circ$.

For $z > b$,

$$\frac{dA}{dz} = 0. \tag{19}$$

We further have

$$\frac{d\Phi}{dz} = 0, \tag{20}$$

$$\frac{dX}{dz} = \frac{dA}{dz}\cos\Phi, \tag{21}$$

$$\frac{dY}{dz} = \frac{dA}{dz}\sin\Phi, \tag{22}$$

$$\frac{dZ}{dz} = 1. \tag{23}$$

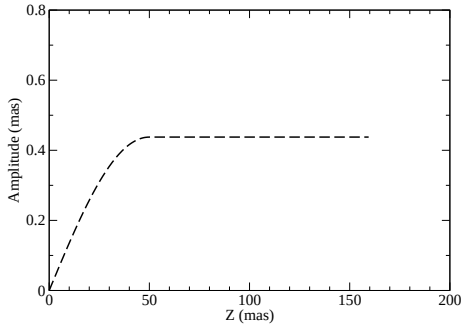

Fig. 3 Assumed amplitude function $A(z)$ for describing the trajectory.

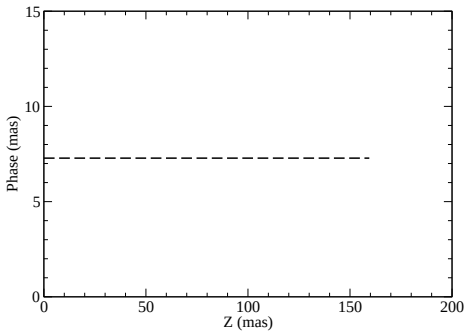

Fig. 4 Assumed phase function $\Phi(z)$ for describing the trajectory. Here $\Phi = 7.283$ rad, corresponding to a precession phase $\phi = 3.5$ rad.

Thus from Equations (9), (10) and (14) we have

$$\Delta = \arctan\Big(\frac{dA}{dz}\Big), \tag{24}$$

$$\Delta_p = \arctan\Big(\frac{dA}{dz}\sin\Phi\Big), \tag{25}$$

$$\Delta_s = \arccos\left(\left[1+\left(\frac{dA}{dz}\right)^2\right]^{-1/2}\right). \tag{26}$$

$$\tag{27}$$

Substituting Δ, Δ_p and Δ_s into Equations (8) and (11)–(13), we can calculate the viewing angle θ, $\beta_{\rm a}$, δ and T'.

5 PROPERTIES OF THE MODEL

To finally define a specific model, we still have three parameters to be set: angles ε and ψ and the collimation parameter b. We take $\varepsilon = 1.32°$, $\psi = 28.53°$, and $b = 50$ mas. The functions $A(z)$ and Φ are shown in Figures 3 and 4. The results can be described as follows.

5.1 Initial PA-ϕ Relation

The model predicts a relation between the ejection (or initial) position angle and the precession phase ϕ. The result is given in Table 1 and shown in Figure 5. The curve shows the change of the initial position angle in one precession cycle, which has an asymmetrical shape and a range of $\sim 70°$, and is consistent with the observational data (Chatterjee et al. 2008, see below).

The model also gives the change of initial viewing angle in one precession cycle. The relation between the initial viewing angle and the precession phase ϕ is shown in Figure 6. It can be seen that the initial viewing angle changes between $0.54°$ and $2.1°$. This is consistent with the small-angle solution suggested by Homan et al. (2003) for explaining the kinematics of knot C4 and the viewing angles derived from other superluminal knots (Chatterjee et al. 2008). Correspondingly, the opening angle of the precession cone is $1.56°$.

Table 1 Precession Model: Precession Phase ϕ and Initial Position Angle

Phase ϕ (rad)	PA (°)	Phase ϕ (rad)	PA (°)
0.0	–137.9	3.75	–95.1
0.5	–127.7	4.0	–112.6
1.0	–117.0	4.25	–133.0
1.5	–106.4	4.5	–147.0
2.0	–96.4	4.75	–153.5
2.25	–91.8	5.0	–155.2
2.5	–87.7	5.25	–154.1
2.75	–84.4	5.5	–151.4
3.0	–82.3	6.0	–143.3
3.25	–82.2	6.2832	–137.9
3.5	–85.6	6.7832	–127.7

5.2 Distribution of Trajectory

The distribution of the trajectories predicted by the model is shown in Figure 7, which clearly demonstrates the effects of the precession and the collimation of the trajectories for the precession phases $\phi = 6.0$, 5.0, 4.5, 4.0, 3.5, and 2.5 rad. All the paths approach the common position angle at $\sim -125^\circ$ at large core-distances.

5.3 Fit to the Trajectory of Knot C4

In order to fit the trajectory of knot C4, we should consider that at a core distance larger than $\simeq$3 mas, the associated trajectory changed direction due to re-collimation resulting from the interaction of the knot with the boundary between the jet-flow and the interstellar medium (Homan et al. 2003; Jorstad et al. 2005) and thus we need to use a different formula to describe its trajectory beyond the core-distance $\gtrsim$3 mas. In Figure 8 is shown a model-fit to the trajectory of knot C4 by fitting the precession phase $\phi = 3.75$ rad ($\Phi = 7.533$ rad) and a specified amplitude function: when $z < 160$ mas it is represented by Equations (15)–(16) and when $z > 160$ mas it is described by a linearly decreasing function:

$$A(z) = (1.375\times10^{-2})\frac{2b}{\pi}\Big(1 - \frac{z-160}{10}\Big). \tag{28}$$

It can be seen that the model fit for its trajectory is very consistent with the observation by Homan et al. (2003). From Figure 5, it can be seen that the initial viewing angle for knot C4 is about 0.8°, which is also consistent with the results ($\leq 1^\circ$) of Homan et al. In fact, the trajectory of knot C4 is continuously curved as shown in Jorstad et al. (2005), but the above fit, with a broken straight line for core-distance greater than $\sim$3 mas, is good enough. We would mention here that the kinematics (variation of apparent velocity and core-distance with time) of C4 predicted by our model is also consistent with the VLBI observations (Homan et al. 2003). We will study the model-fitting of the kinematics for C4 and other superluminal knots in 3C 279 (trajectory, core-distance and apparent speed) in another paper.

6 MODEL-FITTING RESULTS

6.1 VLBI Data from Literature

3C 279 has been observed with VLBI since the 1970s and we can use the VLBI data that have been available for over 30 yr. In order to search for a precession period, we will try to make a fit to the long-term change of position angle observed for the VLBI knots and the inner-jet position angle defined by Chatterjee et al. (2008). From the literature, we have the following VLBI data.

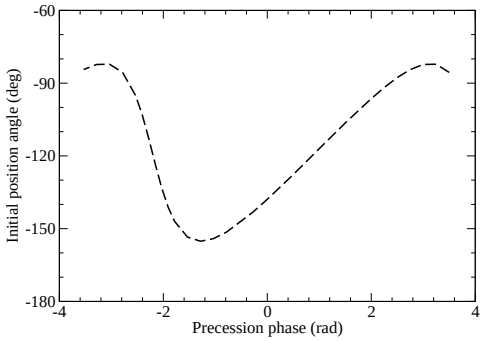

Fig. 5 Relation of the initial position angle and the precession phase ϕ obtained from the proposed precession model. Note that the maximum separation between two extreme position angles corresponds to a difference of precession phase of $\sim$4.3 rad and $\sim$2 rad.

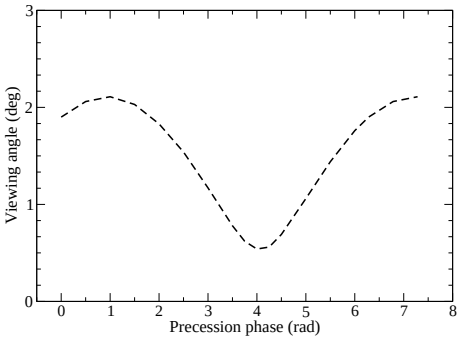

Fig. 6 Relation of the initial viewing angle θ and the precession phase ϕ obtained from the proposed precession model.

– Chatterjee et al. (2008) define the inner-jet position angle with respect to the core as that of the brightest component within 0.1–0.3 mas of the core. As seen from their figure 6, this position angle changes significantly (about 80°) over the $\sim$11 yr VLBI monitoring period. The change in the inner-jet position angle may be used as a complement to the change in ejection position angle (see Fig. 1).
– The position angles averaged within 1 mas of the core for knots (C8–C23) from Chatterjee et al. (2008, their table 5) are used. These values may be regarded as representative for the ejection position angles.
– Larionov et al. (2008) have given the data for knot C24. Its ejection time and position angle are 2006.89$\pm$0.11 and $-120^\circ\pm5^\circ$ respectively. In Figure 1 are shown these VLBI data which indicate that the position angle of the inner jet and the position angle of the ejection of the knots show a similar change with time. The asymmetry of the long-term trend might imply a possible precession of the jet.
– For knots from earlier times (knots C3, C4, C5, C5a, C6, C7 and C7a), the VLBI data of ejection time and initial position angle are collected from

(1) C7a from Jorstad et al. (2004): 1994.67$\pm$0.1 and $-121.0^\circ\pm2.1^\circ$.
(2) C5a, C6 and C7 are taken from Wehrle et al. (2001): (1990.88$\pm$0.3, $-124.7^\circ\pm6^\circ$); (1992.09$\pm$0.15, $-128.9^\circ\pm3^\circ$) and (1993.26$\pm$0.13,$-129.2^\circ\pm2^\circ$).
(3) For C5 from Abraham & Carrara (1998)[1]: 1987.0$\pm$1 and $-84^\circ\pm10^\circ$.
(4) For knot C4 from Wehrle et al. (2001) and Homan et al. (2003): (1984.7$\pm$0.3, $-114^\circ\pm1$), we point out that the position angle at -114° is not the ejection position angle but the position angle at core-distances of about 1–3 mas. Thus in the model-fitting, we should assume an appropriate ejection (initial) position angle and make the initial trajectory approach this position angle at the corresponding core distances.
(5) For knot C3 from Unwin et al. (1989) we have 1972.6$\pm$1 and $-134^\circ\pm10^\circ$.

All these are summarized in Table 2.

[1] The knot C5 designated by Abraham & Carrara is not the same component designated by Wehrle et al. 2001.

Table 2 Ejection Position Angle and Ejection Epoch for Seven Knots

Knot	Ejection time	Ejection PA (°)	Reference
C3	1972.6±1.1	–134±(10)	Unwin et al. 1989
C4	1984.7±0.3	–114±1	Wehrle et al. 2001; Homan et al. 2003
C5	1987.0±1	–84±10	Abraham & Carrara 1998
C5a	1990.88±0.3	–124.7±6	Wehrle et al. 2001
C6	1992.09±0.15	–128.9±3	Wehrle et al. 2001
C7	1993.26±0.13	–129.2±2	Wehrle et al. 2001
C7a	1994.67±(0.1)	–121.0±2.1	Jorstad et al. 2004

Table 3 Precession Model for 25 yr Period: Relation of Ejection Epoch and Phase

Phase ϕ (rad)	Ejection epoch (yr)	Phase ϕ (rad)	Ejection epoch (yr)
6.2832	1973.29	–0.2832	1999.42
6.0	1974.42	–0.7832	2001.41
5.5	1976.41	–1.0332	2002.40
5.25	1977.40	–1.2832	2003.40
5.0	1978.40	–1.5332	2004.39
4.75	1979.39	–1.7832	2005.39
4.5	1980.39	–2.0332	2006.38
4.25	1981.38	–2.2832	2007.38
4.0	1982.38	–2.5332	2008.37
3.75	1983.37	–2.7832	2009.37
3.5	1984.37	–3.0332	2010.36
3.25	1985.36	–3.2832	2011.36
3.0	1986.36	–3.5332	2012.35
2.75	1987.35	–3.7832	2013.35
2.5	1988.35	–4.0332	2014.34
2.25	1989.34	–4.2832	2015.34
2.0	1990.34	–4.7832	2017.33
1.5	1992.33	–5.2832	2019.32
1.0	1994.32	–5.7832	2021.30
0.5	1996.30	–6.2832	2023.29
0.0	1998.29		

In addition, we will choose a few periods from 15 yr to 30 yr to fit the observational data with the starting point set at (2003.40, PA=$-155°$), which correspond to the observational data for knot C20 as given by Chatterjee et al. (2008).

The model-fitting results we obtain are shown in Figures 9–14.

The ejection epoch is given by

$$T(\mathrm{yr}) = 2003.40 - \frac{T_\mathrm{p}}{2\pi}(\phi + 1.2832), \tag{29}$$

where T_p is the precession period (yr) to be chosen. We choose ejection phase $\phi = -1.2832$ rad (or +5.0 rad) as a reference point which corresponds to the ejection epoch 2003.40 of knot C20 and the observed minimum position angle ($-155°$).

6.2 Model-fitting of Inner-jet and Ejection Position Angles

In Figures 9–12 are shown the model-fits to the observed change of the inner-jet position angle defined by Chatterjee et al. (2008) (data points shown by diamonds) and the earlier data for C3 to C7a by the model with the precession periods 15, 20, 25 and 30 yr, respectively. Here we should point out that in these plots, the epoch is measured along the direction opposite to that of the precession phase, that is, increasing time corresponds to a decrease in the phase.

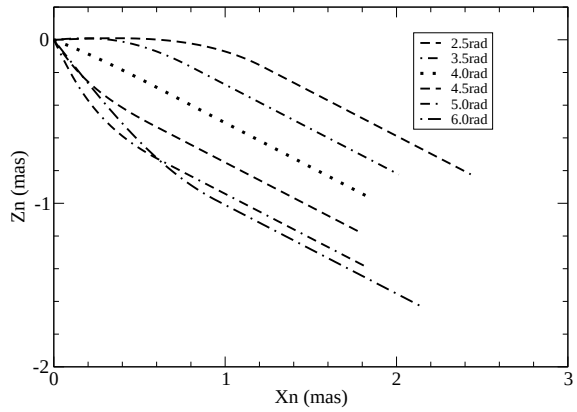

Fig. 7 Distribution of the model trajectories for precession angles $\phi = 2.5$, 3.5, 4.0, 4.5, 5.0 and 6.0 rad (for $z \leq 110$ mas). Note that at core-distances larger than $\sim$0.3–0.5 mas, the trajectory of individual knots often deviates from those shown here, probably due to intrinsic curved motion or interactions between the knots and their environment.

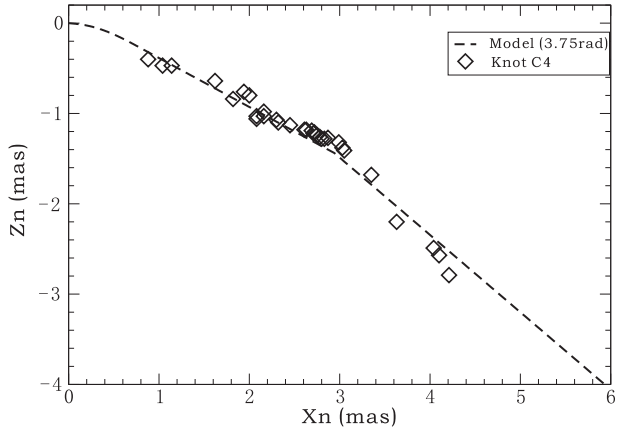

Fig. 8 Model-fit to the observed trajectory of knot C4. The model amplitude is given by Eqs. (15), (16) and (27) with a path-break at $z = 160$ mas. Precession phase $\phi = 3.75$ rad. Note that the non-ballistic trajectory near the core has an initial ejection position angle of $\sim -95^\circ$, different from the observationally derived value by Homan et al. (2003).

By visual inspection, it can be seen from Figures 9 to 12 that for the fits to the inner-jet position angles, the four models are similar to each other and they all roughly follow the long-term trend of the observed change. Thus the ejection position angles for C3, C4, C5, C5a, C6, C7 and C7a are crucial for the test of the models. Inspecting the four model-fits, we can see that the model with a precession period of 25 yr seems better (than others) to be considered as an acceptable fit, because for this period the ejection position angles of knots C3, C5 and C7a are already consistently well-fitted (Fig. 11). These model-fitting results are shown more clearly in Figures 13 and 14, in which the position angle

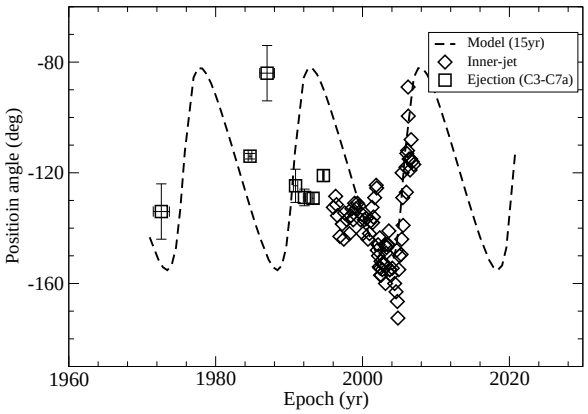

Fig. 9 Model-fit to the inner-jet position angle of 3C 279 for a precession period of 15 yr. Data are from Chatterjee et al. 2008 plus those data collected from literature. Diamonds–inner jet position angle; squares–ejection position angles for C3 to C7a (see Table 2).

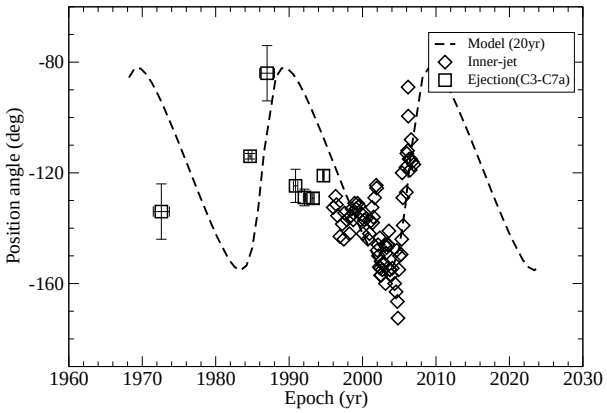

Fig. 10 Same as in Fig. 9, but for a precession period of 20 yr.

of knot C4 is also well-fitted by correcting its non-ballistic motion near the core. For knot C4, as we have seen from Figure 8, its trajectory at a core-distance larger than $\sim$1 mas is well-fitted by our precession model defined by precession phase ϕ=3.75 rad, which has an ejection position angle at $\sim -95^\circ$ and gradually approaches the position angle $\sim -114^\circ$ at a core-distance $\sim 1-3$ mas. This means that the data-point for C4 should be (1983.4, -95°) instead of the observationally derived (1984.7, -114°), thus it is situated right on the model curve (see Figs. 13–14). The model also well fits its kinematics (apparent speed, variation in core-distance and viewing angle with time, Lorentz factor and Doppler beaming, derived by Homan et al. 2003). We will discuss the model-fits to the kinematics of several knots in detail in a separate paper.

We also point out that the position angle of knot C20 (as a fiducial point) is very consistent with the 25-yr period. Knots C23 and C24 are on the increasing branch of the change in position

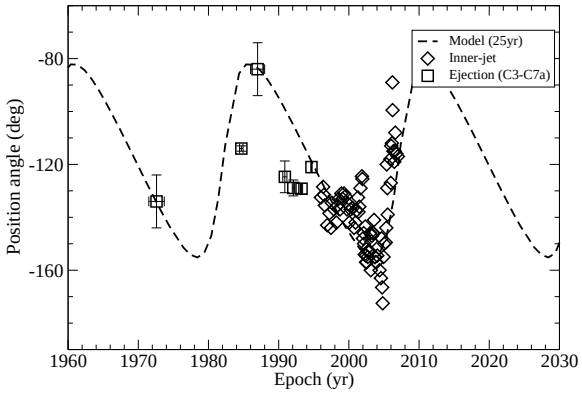

Fig. 11 Same as in Fig. 9, but for a precession period of 25 yr.

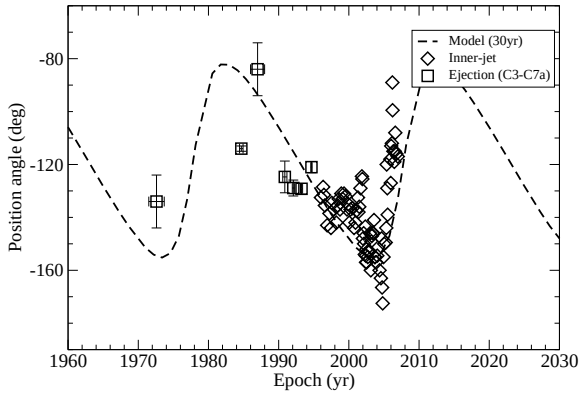

Fig. 12 Same as Fig. 9, but for a precession period of 30 yr.

angle with time (Fig. 14). Also, the position angle observed for C24 (Larionov et al. 2008; Jorstad 2010: private communication) is consistent with the model, but that for knot C23 is not, deviating from the model-curve (Fig. 14) by about $\sim 15^\circ$. One possibility might be that knot C23 had already deviated from its initial ejection trajectory within a core-distance of 0.1 mas. (Note that in our model, the initial viewing angle of knot C23 is $\sim 0.5^\circ$, corresponding to an axial distance of about 60 pc). Similar cases could exist for knots C12–C15: their position angles observed at the earliest epochs are more consistent with the model than their average position angles within 1 mas. In Table 3 the relation between the ejection epoch and the precession phase for the precession model of 25 yr is given.

Thus we find that the jet-nozzle precession model with a period of 25 yr can fit the observed long-term trend of the change in position angle over the period 1972 to 2007. The inclusion of the observed ejection position angles of knots C3, C4 and C5 is significant, extending the fit to more than one cycle. Based on this 25yr periodicity, we predict that superluminal knots would be ejected at position angles around $\sim -90^\circ$ in 2010–2012.

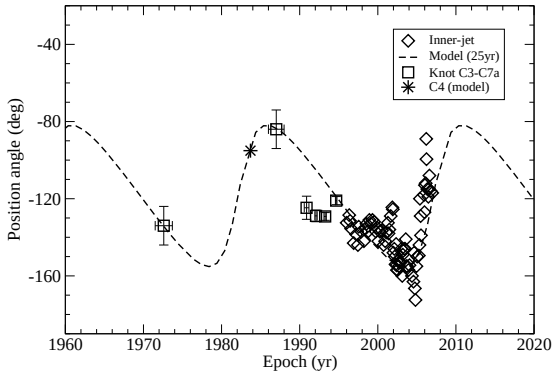

Fig. 13 Same as Fig. 11, but with correction of the ejection epoch and initial ejection position angle for knot C4 (denoted by an asterisk).

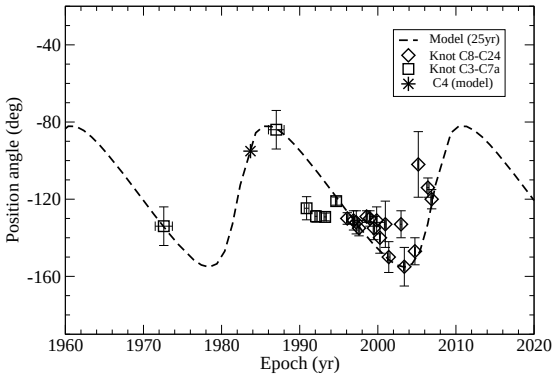

Fig. 14 Fit of the ejection position angles of superluminal components C3 to C24 by the jet-nozzle precession model with a period of 25 yr. For knot C4, the ejection position angle and ejection epoch have been "corrected" to $(-95.1^\circ, 1983.4)$ instead of the observationally derived values $(-114^\circ, 1984.7)$ according to our precession model. It is denoted by an asterisk.

7 DISCUSSION AND CONCLUSIONS

In the above we have shown that the long-term (longer than 10 yr) wobbling of the position angle of the superluminal knots observed in 3C 279 could be interpreted by a jet-nozzle precession model, in which the knots move along a common collimated jet channel precessing with a period of $\sim$25 yr. However, the observed short-term (less than 1–2 yr) swings or fluctuations in position angle cause some uncertainties. Specifically, we have obtained the following results.

– The long-term trend of the variation in the position angles of the superluminal knots could be obtained from a periodic variation of the precession phase ϕ of a fixed collimated channel defined by $(A(z),\ \Phi)$ given in Equations (15)–(17). The model is established for very small

viewing angles (less than 2°) and thus can be consistent with the apparent motions obtained by VLBI observations. This collimated precessing jet nozzle model is different from the usually adopted ballistic precession models (see Tateyama & Kingham 2004).

- We obtain the relation between the ejection position angle and the precession phase ϕ ($\phi = \Phi - 3.738$). The derived precession period is $\sim$25 yr in the observer's frame (~ 16.3 yr in the galaxy frame). The model could fit the trends of the changes in both the ejection position angle of the superluminal knots and the inner-jet position angle defined by Chatterjee et al. (2008). It is shown that the data-points for knots C3, C4 and C5 are well-fitted. For knot C4, non-ballistic motion near the core has been corrected. (The model-fits of the kinematics of the superluminal knots will be discussed in another paper).
- The axis of the jet-nozzle precession is found to make an angle of 88.68° with the sky-plane (or the angle between the precession axis and the direction toward the observer is $\varepsilon = 1.32^\circ$). The azimuthal angle of the precession axis in the sky plane is 28.53° (calculated from north to east). The half opening angle of the precession cone (η) is very small: η=0.78°.
- The initial viewing angle varies during the precession between 0.54° and 2.1° (as shown in Fig. 6). Such very small viewing angles are consistent with the derivations from the analysis of kinematics observed by VLBI (e.g. see Homan et al. 2003; Jorstad et al. 2004).
- If our model is applicable, we predict that the ejection position angle would approach $\sim -90^\circ \pm 10^\circ$ in 2010–2012. This might be the most important test. It seems that there is still some room for improvement in the determination of the period.
- The short-term swings of the inner-jet position angle and the initial ejection position angle of the knots remain to be investigated. VLBI astrometric observations of the core position with respect to some nearby stationary radio object would be needed to show whether this phenomenon is due to the motion of the 'presumably stationary' core or not. Also for the case of the viewing angle being very small (less than 2°) in 3C 279, space-based mm-VLBI observations would be needed to detect the initial position angle at 0.01 mas resolution and solve the origin of the wobbling of the jet's position angle.

As Jorstad & Marscher (2005) pointed out, in 3C 279 both the Lorentz factor and the viewing angle of the components vary significantly and the variations have random characters. These can be produced as the result of magneto-hydrodynamical instabilities in accretion disk-jet driven systems (e.g. Hardee & Rosen 1999; McKinney 2006). However, it seems possible that the long-term variability of the wobbling of the position angle on time scales $>$10 yr might be governed by the jet-nozzle precession (Agudo 2009). Most likely both mechanisms operate, so that the Lorentz factor can reach up to 25–30 (with Doppler factor as high as 45–50), varying on timescales as short as a few months. These parameters are consistent with the high amplitude variability of the quasar from radio wavelengths to γ-ray energies.

In summary, our results are similar to the case for the quasar 3C 345, in which the change of the ejection position angle of superluminal knots could be fitted by the precession of a steady ejection channel (Qian et al. 2009). Thus, it appears possible that in both 3C 279 and 3C 345, some general mechanisms exist for producing jet nozzle precession and formation of a steady ejection channel.

Steady helical and collimated channels might be formed through magneto-hydrodynamic processes (Begelman et al. 1980; Camenzind 1990; Blandford & Payne 1982; Blandford 1994; Daly & Marscher 1988; Vlahakis & Koenigl 2004). The origin of wobbling in blazar jets is still not clear. Jet nozzle precession might be one of the alternative interpretations, as proposed in this paper for the long-term variations in position angle observed in 3C 279, except that jet wobbling is caused by more erratic jet instabilities in the innermost region itself; a precession model would imply that the jet-nozzle precession is associated with the magneto-hydodynamic processes in the central engine (black-hole/accretion disk system). It is most probable that jet wobbling is caused by the precession of the accretion disk of the primary black hole, which is driven by torques induced by a companion

black hole (Katz 1997; Lister et al. 2003; Stirling et al. 2003), or by the gravitational Bardeen-Peterson effect (Liu & Melia 2002; Caproni et al. 2006). Scenarios of jet-nozzle precession caused by binary motion seem not to be preferred, since they predict jet wobbling timescales too long to be compared with the observed ones (Lobanov & Roland 2005). However, the results of this paper might provide more specific evidence for a regular and steady structure at the base of the inner jet. Such physical structures should try to be observed in the electromagnetically dominated zones of blazars with the next generation of space-based mm-VLBI techniques (Jorstad et al. 2007; Marscher 2009; Agudo 2009).

Acknowledgements I wish to thank Dr. S. G. Jorstad (Boston University, USA) for providing the data on the trajectory of knots C23 and C24. I also thank Gan Hengqian and Gao Long for their helpful discussion.

References

Abraham, Z., & Carrara, E. A. 1998, ApJ, 496, 172
Agudo, I., Bach, U., Krichbaum, T. P., et al. 2007, A&A, 476, L17
Agudo, I. 2009, in Approaching Micro-Arcsecond Resolution with VSOP-2: Astrophysics and Technology (ASPCS 402), eds. Y.Hagiwara, E. Fomalont, H. Tsuboi, & Y. Murata, 330
Bartel, N., Herring, T. A., Ratner, M. I., et al. 1986, Nature, 319, 733
Begelman, M. C., Blandford, R. D., & Rees, M. J. 1980, Nature, 287, 307
Blandford, R. D., & Payne, D. G. 1982, MNRAS, 199, 883
Blandford, R. 1994, in ASP Conf. Ser. 54, The physics of Active Galaxies, eds. G. V. Bicknell, M. A. Dopita, & P. J. Quinn, 23
Camenzind, M. 1990, in IAU Symp. 140, Galactic and Intergalactic Magnetic Fields, eds. R. Beck et al., 413
Caproni, A., Livio, M., Abraham, Z., & Cuesta, H. J. M. 2006, ApJ, 653, 112
Carrara, E. A., Abraham, Z., Unwin, S. C., & Zensus, J. A. 1993, A&A, 279, 83
Chatterjee, R., Jorstad, S. G., Marscher, A. P., et al. 2008, ApJ, 689, 79
Cohen, M. H., Cannon, W., Purcell, G. H., & Shaffer, D. B. 1971, ApJ, 170, 207
Cotton, W. D., Counselman III, C. C., Geller, R. B., et al. 1979, ApJ, 229, L115
Daly, R. A., & Marscher, A. P. 1988, ApJ, 334, 539
Hardee, P. E., & Rosen, A. 1999, ApJ, 524, 650
Hartman, R. C., Bertsch, D. L., Fichtel, C. E., et al. 1992, ApJ, 385, L1
Hogg, D. W. 1999, astro-ph/9905116
Homan, D. C., Lister, M. L., Kellermann, K. I., et al. 2003, ApJ, 589, L9
Jorstad, S. G., & Marscher, A. P. 2005, Mem. S. A. It. 76, 106
Jorstad, S. G., Marscher, A. P., Lister, M. L., et al. 2004, AJ, 127, 3115
Jorstad, S. G., Marscher, A. P., Lister, M. L., et al. 2005, AJ, 130, 1418
Jorstad, S. G., Marscher, A. P., Stevens, J. A., et al. 2007, AJ, 134, 799
Katz, J. I. 1997, ApJ, 478, 527
Klare, J., Zensus, J. A., Lobanov, A. P., Ros, E., Krichbaum, T. P., & Witzel, A. 2005, in ASP Conf. Ser. 340, Future Directions in High Resolution Astronomy, eds. J. D. Romney, & M. J. Reid, 40
Klare, J. 2003, PhD. Thesis, Quasi-Periodicity in the Parsec-Scale Jet of the Quasar 3C 345 (A High Resolution Study Using VSOP and VLBA), Rheinischen Friedrich-Wilhelms-Universitat (Germany: Bonn), *http://thesis.jensklare.com*
Kudryavtseva, N. A., & Pyatunina, T. B. 2006, Astronomy Report, 50, 1
Larionov, V. M., Jorstad, S. G., Marscher, A. P., et al. 2008, A&A, 492,289
Lister, M. L., Kellermann, K. I., Vermeulen, R. C., et al. 2003, ApJ, 584, 135
Liu, S., & Melia, F. 2002, ApJ, 573, L23

Lobanov, A. P., & Roland, J. 2005, A&A, 431, 831
Marscher, A. P. 2008, in ASP Conf. Ser. 386, Extragalactic Jets: Theory and Observation from Radio to Gamma-Ray, eds. J. A. Rector, & D. S. De Young, 437
Marscher, A. P. 2009, in ASP Conf. Ser. 402, Approaching Micro-Arcsecond Resolution with VSP-2: Astrophysics and Technologies, eds., Y. Hagiwara, Ed Fomalont, M. Tsuboi, & Y. Murata, 194
McKinney, J. C. 2006, MNRAS, 368, 1561
Pen U. L. 1999, ApJS, 120, 49
Qian, S. J., Witzel, A., Zensus, J. A., et al. 2009, RAA (Research in Astronomy and Astrophysics), 9, 137
Qian, S. J., Witzel, A., Krichbaum, T., Quirrenbach, A., Hummel, C. A., & Zensus, J. A. 1991, Acta Astron. Sin. 32, 369 (English translation: in Chin. Astro. Astrophys. 16, 137)
Qian, S. J., Kudryavtseva, N. A., Britzen, S., Krichbaum, T. P., Gao, L., Witzel, A., Zensus, J. A., Aller, M. F., Aller, A. D., & Zhang, X. Z. 2007, ChJAA (Chin. J. Astron. Astrophys.), 7, 364
Spergel, D. N., Verde, L., Peiris, H. V., et al. 2003, ApJS, 148, 175
Stirling, A. M., Cawthorne, T. V., Stevens, J. A., et al. 2003, MNRAS, 341, 405
Tateyama, C. E., & Kingham, K. A. 2004, ApJ, 608, 149
Unwin, S. C., Cohen, M. H., Birreta, J. A., et al. 1989, ApJ, 340, 117
Valtonen, M. J., Lehto, H. J., Sillanpää, A., et al. 2006, ApJ, 646, 36
Valtonen, M. J., Lehto, H. J., Nilsson, K., et al. 2008, Nature, 452, 851
Vlahakis, N., & Koenigl, A. 2004, ApJ, 605, 656
Wehrle, A. E., Piner, B. G., Unwin, S. C., et al. 2001, ApJS, 133, 297
Whitney, A. R., Shapiro, I. I., Rogers, A. E. E., et al. 1971, Science, 173, 225